

INFLUENCE OF THE PLAN DENSITY OF A CUBE-BASED CANOPY ON THE STRUCTURE OF THE LOWER ATMOSPHERIC BOUNDARY LAYER

Laurent PERRET
 LHEEA

UMR 6598 CNRS Centrale Nantes
 Nantes, France
 laurent.perret@ec-nantes.fr

Romain MATHIS
 IMFT

Université de Toulouse, CNRS, INPT, UPS
 Toulouse, France
 romain.mathis@imft.fr

Jérémy BASLEY

Dept. of Aeronautics
 Imperial College
 London, UK
 j.basley@imperial.ac.uk

ABSTRACT

An experimental investigation of the structure of the boundary-layer developing over an urban-like rough wall is performed considering wall configurations that represent three idealised urban terrains. Both stereoscopic particle image velocimetry and two-point hot-wire data are investigated through one- and two-dimensional spectral analysis. It is shown that the flow characteristics within the inertial layer appear to be independent from the wall configuration. This region is populated with coherent structures of the same type as those found in smooth-wall flows, namely very large-scale motions and large-scale motions, the later showing self-similar features. These coherent structures, whose footprint is mainly visible on the streamwise and spanwise velocity components, also appear to be present in the roughness sublayer. Within the roughness sublayer, the influence of the canopy density shows in the characteristics of the wall-normal velocity component w . The most energetic scales in the auto-spectra of w and in the co-spectra between u and w are indeed of the same order of magnitude as the roughness obstacle size and decrease with increasing density. Instead of varying progressively with the packing density, they appear to be constrained by the presence of the canopy for the densest investigated configurations consistently with the change of the flow regime reported in the literature.

INTRODUCTION

The vertical structure of turbulent boundary layers developing over dense canopies is strongly impacted, at least in its lower part, by the presence of the roughness obstacles (Jiménez, 2004). The presence of roughness elements on the wall not only alters drastically the near-wall turbulent cycle, but also imposes scales of the order of the canopy height within the flow. Therefore, if the height of the roughness elements is larger than a few wall units, roughness is expected to influence the entire boundary layer struc-

Table 1. Characteristics of the boundary layer for the three canopies, where U_τ is the friction velocity, ν the kinematic viscosity and superscript + denoting the inner scaling based on U_τ and length scale ν/U_τ .

λ_p	U_e (m/s)	U_τ (m/s)	δ/h	δ^+	h^+
6.25%	5.62	0.40	22.4	29 600	1320
25%	5.73	0.42	22.7	32 200	1420
44.4%	5.60	0.36	21.0	24 500	1170

ture (Jiménez, 2004). In the context of wind flows in urban areas, the influence of the canopy has been shown to be strongly dependent on the height of the obstacles, their arrangement and their spacing. The aim of the present work is to study the influence of varying the plan density λ_p (see Fig 1, bottom, for definition of λ_p) of a staggered cube array modelling the urban canopy on the dynamics of the flow via a detailed analysis of its spectral characteristics. Three values of $\lambda_p = 6.25, 25$ and 44.4% are chosen to cover the three different flow regimes highlighted by Grimmond & Oke (1999), namely the *isolated*, *wake-interference* and *skimming flow regimes* (see Fig. 1, bottom), in order to investigate (i) the influence of the roughness geometry and the variation of the near-wall flow regime on the structure of the flow within the logarithmic layer, (ii) the importance and the footprint of the roughness element dimension on the typical scales of the flow in the roughness sublayer (RSL), and (iii) the effect of varying the obstacle spacing on the structure of the flow within the RSL.

EXPERIMENTAL SETUP

The experiments were conducted in the wind tunnel of the LHEEA, Nantes, France, which has a working section of dimensions $24 \text{ m} \times 2 \text{ m} \times 2 \text{ m}$ (Fig. 1, top). To model the urban boundary layer at high Reynolds number (Tab. 1), a combination of five tapered spires, a fence and a 22 m long fetch of staggered cubes of height $h = 50 \text{ mm}$ is

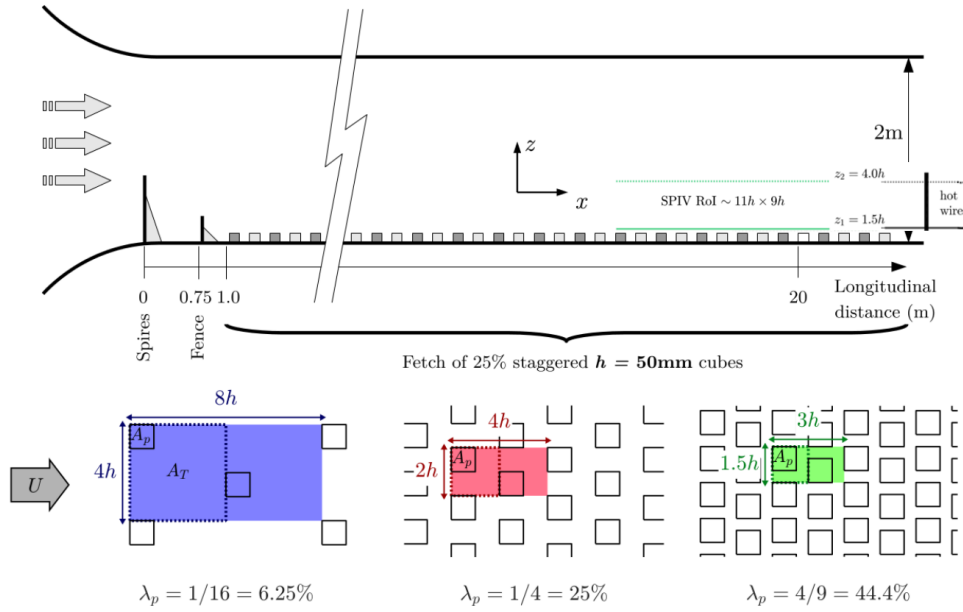


Figure 1. Experimental setup: (top) atmospheric wind-tunnel, (bottom) top-view sketch of the three canopies. The shaded region represents the periodic pattern for each case; the area A_T such that $\lambda_p = A_p/A_T$ is delimited by dotted contours.

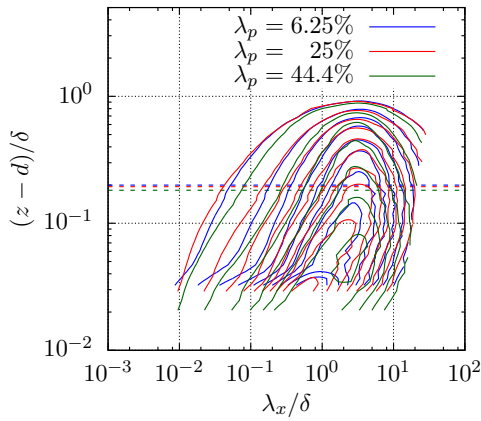


Figure 2. Wall-normal distribution of the pre-multiplied energy spectra $k_x S(u, u) / U_f^2$. The horizontal dashed lines show the wall-normal location $z_f = 5h$ for each flow configuration. Pre-multiplied energy spectra contours have been smoothed on a logarithmically distributed frequency grid and are shown with an increment of 0.2, from 0.2 to 2.8.

employed (see Basley *et al.*, 2018, for full details). Flow measurements have been undertaken at two wall-normal locations, $z_1 = 1.5h$ and $z_2 = 4h$, using three-component-two-dimensional Stereoscopic Particle Image Velocimetry (SPIV) in a streamwise-spanwise plane (Fig. 1, top). These two locations lie within the RSL and in the inertial region, respectively (Basley *et al.*, 2018). The streamwise extent and acquisition frequency of the SPIV velocity fields are such that they can be stitched in the streamwise direction by applying Taylor's hypothesis (see Basley *et al.*, 2018). This SPIV is complemented by two-point single-HWA measurements performed in the RSL and the inertial layer with a fixed point at $z_f = 5h$ and a moving probe at $1.25h < z_m < 4h$ (Perret *et al.*, 2019). These data are used to compute the spectral coherence in this region.

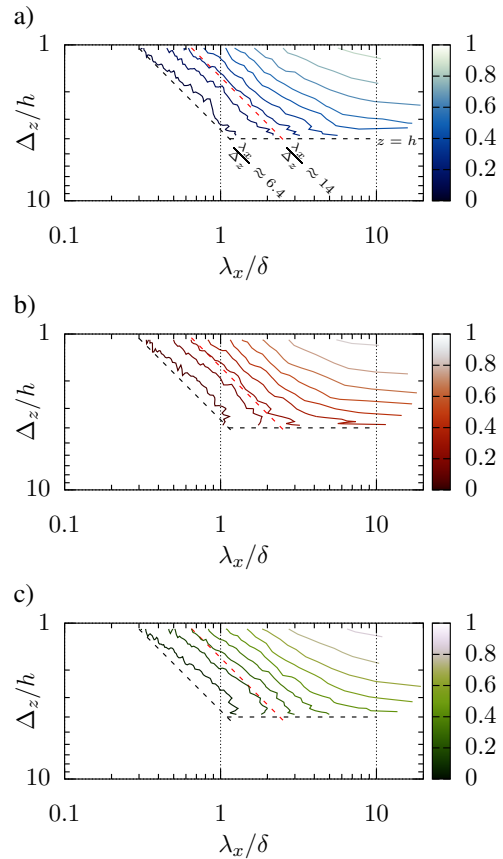


Figure 3. Spectrograms of coherence $\gamma^2(\Delta_z, \lambda_x)$ for $\lambda_p =$ (a) 6.25%, (b) 25% and (c) 44.4% with contours from 0.05 to 0.85 with an increment of 0.1. Dashed lines represent two λ_x / Δ_z ratios, described in (a).

RESULTS AND DISCUSSION

Two-point HWA data are first analyzed to demonstrate the presence of very large-scale motions (VLSMs) in the outer region of the flow and their superimposition onto the

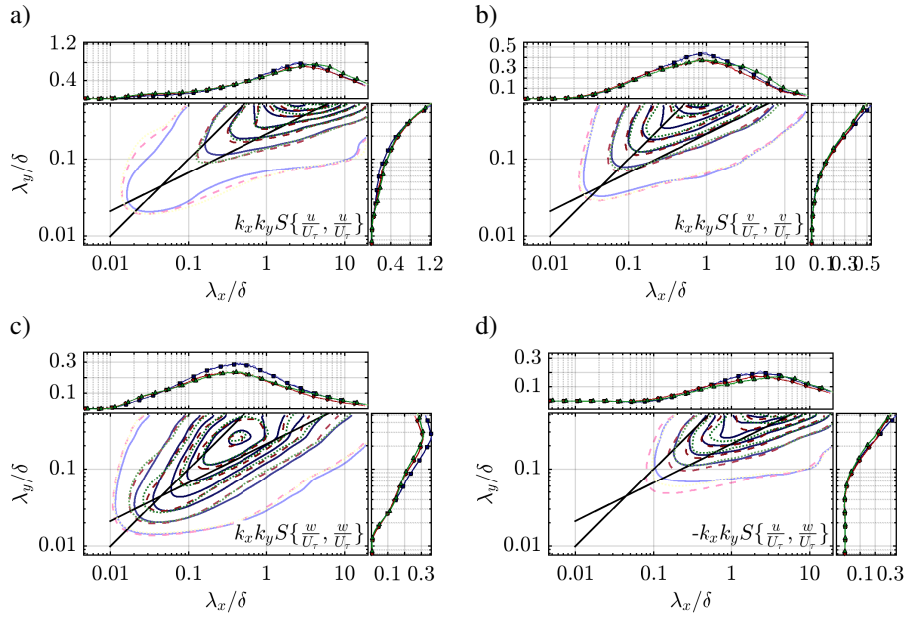


Figure 4. Pre-multiplied spectra in streamwise-spanwise plane located in the logarithmic layer ($z_1 = 4h$) of (a) u , (b) v and (c) w and (d) co-spectra between u and w .

near-canopy turbulence in the RSL. Contour maps of the pre-multiplied energy spectra of the streamwise velocity component u as a function of the wall-normal distance and λ_x are shown in figure 2. For the three investigated canopy densities, contrary to what is observed in smooth-wall configurations at similar Reynolds numbers, it is not possible to distinguish clear maxima associated on one hand with the near-wall turbulence and, on the other hand, with the larger scales existing in the logarithmic layer. The roughness obstacles generate scales much larger than those encountered in the near-wall region in smooth-wall boundary layers, eliminating the expected spectral separation. The overall good agreement between the three different flow configurations above $(z-d)/\delta \approx 0.1$ shows that only the lower part of the flow is affected by the roughness pattern and density. Above this wall-normal location, the most energetic scales correspond to streamwise wavelengths of 3 to 4 δ in agreement with the presence of VLSMs. The wall-normal evolution of the spectral coherence $\gamma^2(z_f, z_m, \lambda_x)$ is presented in figure 3. For all roughness configurations, coherence levels become independent of the considered streamwise wavelength for λ_x/δ larger than approximately 10, in agreement with the presence of VLSMs that span the entire boundary layer depth and range deep near the wall. For smaller wavelengths, the levels of γ^2 are scale-dependent. There is indeed a region where the γ^2 isocontours are linear. This behaviour has been recently linked to the presence of self-similar eddies in the lower part of the boundary-layer by Baars *et al.* (2017). Contrary to what has been shown in smooth-wall flows by these authors, a departure of the isocontours from the straight line behaviour for the lowest levels of coherence at large wall-normal separation Δ_z is noticeable. This might indicate that this range of wavelengths does not correspond to self-similar eddies but to a different type of structures of rather large wall-normal extent (at least $4h$, the maximum probe separation), leaving a weak imprint onto the flow. The near-canopy flow is therefore populated of coexisting coherent structures of different type, the exact characterisation of which remaining an open question given the limited amount of information available from the

present two-point HWA database.

The spectral signature of the flow is further investigated first in the streamwise-spanwise plane located at $z_2 = 4h$, using the Taylor-extended SPIV fluctuating velocity fields. Two-dimensional pre-multiplied (by wave numbers $k_{x,y} = 2\pi/\lambda_{x,y}$) power spectral densities $S(u, u)$, $S(v, v)$ and $S(w, w)$ of the streamwise velocity component, spanwise and wall-normal velocity components, respectively, and the co-spectra uw are shown in figure 4. All spectra and co-spectra obtained at this wall-normal location show a similar spectral signature (figure 4), implying that the influence of the canopy is limited to the RSL and vanishes once above it. In agreement with previous observations, the spectral signature of LSMs is mainly carried by the streamwise velocity and consists of a broad-band peak scaling with δ , centred around $\lambda_x \sim 4\delta$ in the logarithmic layer. The two-dimensional spectrum of u also reflects the anisotropy of the associated structures, the ridge of maximum energy following a line close to $\lambda_x \propto \lambda_y^2$. Low and high momentum regions are therefore elongated structures which are wider as they become longer. The spectrum of the spanwise component shows a peak of energy for $\lambda_x \sim \delta$ while the spectra $S(w, w)$ corresponds to more compact events with a peak at $\lambda_x \sim 0.4\delta$. While the characteristics of the Reynolds shear stress auto-spectra $S(uv, uv)$ (not shown here) seem to be controlled by the most energetic scales of v . The characteristics of $S(w, w)$ and $S(u, w)$ (and $S(uw, uw)$ not shown here) evolve differently and appear to be linked to the presence of ejection and sweep events. In the RSL (at $z_1 = 1.5h$), the main peak in $S(u, u)$ is found at $\lambda_x \sim \delta$ (figure 5 top row) while the peak in $S(v, v)$ is shifted to $\lambda_x \sim 0.2\delta$ (figure 5 bottom row). There seems to be no direct impact of the canopy geometry on the LSMs which leave their footprint mainly in the streamwise and spanwise velocity components u and v , respectively, as the wavelength and amplitude of the peaks in $S(u, u)$ and $S(v, v)$ are similar for the three canopies. As in the logarithmic region, the characteristics of the Reynolds shear stress auto-spectra $S(uv, uv)$ seem to be controlled by the most energetic scales of v (not shown here). However, when comparing the logarithmic layer and

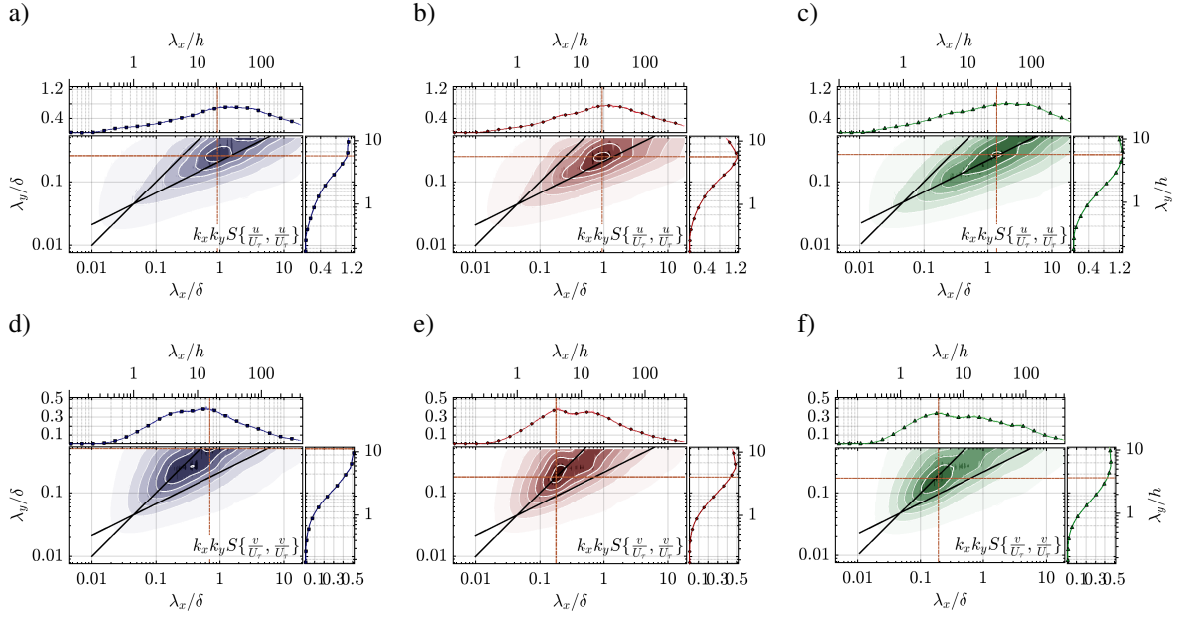


Figure 5. Pre-multiplied spectra in streamwise-spanwise planes in the RSL ($z_1 = 1.5h$) of (top row) u and (bottom row) v . The three canopy configurations with $\lambda_p = 6.25\%$, 25% and 44.4% are shown in the left, center and right columns, respectively.

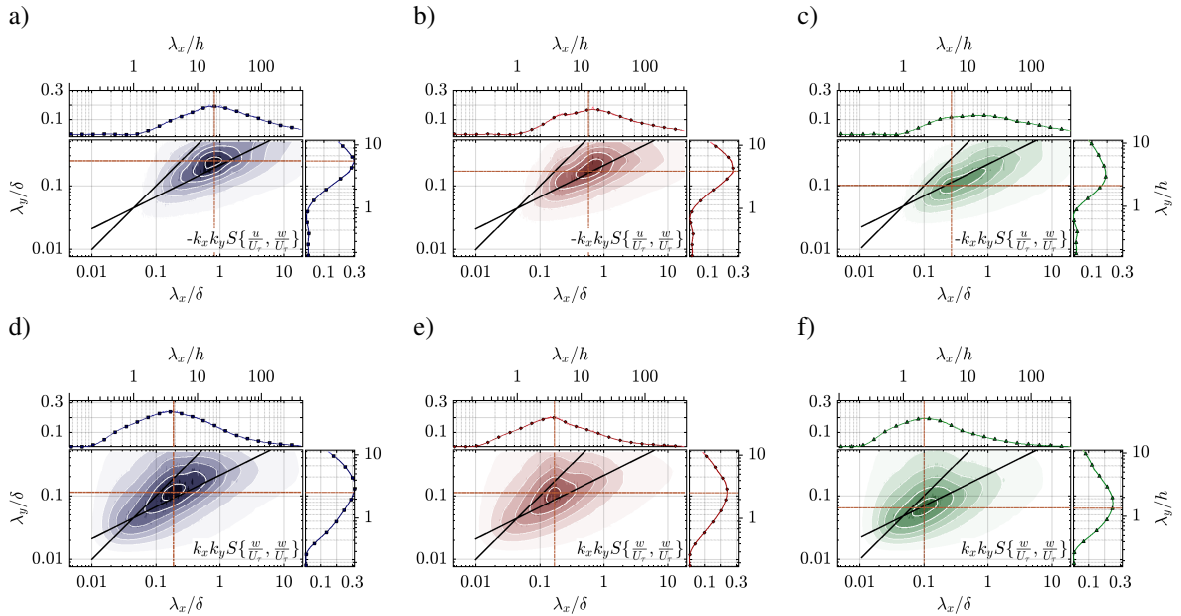


Figure 6. Pre-multiplied (top row) co-spectra between u and w and (bottom row) spectra of w in streamwise-spanwise planes in the RSL ($z_1 = 1.5h$). The three canopy configurations with $\lambda_p = 6.25\%$, 25% and 44.4% are shown in the left, center and right columns, respectively.

the RSL, the two-dimensional auto-spectra at $z_1 = 1.5h$ of u and v show the emergence of a secondary peak of slightly smaller energy at larger wavelength in both directions x and y . The emergence of this secondary peak, clearly noticeable in the two-dimensional spectra, is not as visible in the one-dimensional statistics, leading rather to a broader and flatter peak. This suggests that the larger structures existing in the logarithmic layer leave a strong imprint on the flow in the RSL, where exist structures of similar characteristics and energy but of smaller scales.

Pre-multiplied spectra of the wall-normal velocity component w and co-spectra $-k_x k_y S(u, w)$ between u and w obtained in the RSL are shown in figure 6 (bottom and top row, respectively) in order to identify the scales related to ejection

and sweeps and wall-normal transport of momentum. Auto-spectra $S(w, w)$ exhibit smaller typical scales than the two other velocity components, of the order of h , and dependent on the canopy pattern, showing that w is associated to canopy interactions and near-wall flow dynamics. There is indeed a clear decrease with increasing λ_p of the most energetic scales, going from $(\lambda_x, \lambda_y) \approx (4.5h, 2.5h)$ for $\lambda_p = 6.25\%$, to $(2h, 1.5h)$ for $\lambda_p = 44.4\%$. As far the characteristic spanwise scale is concerned, no clear trend with λ_p (or any characteristic scale of the canopy pattern) has been found, suggesting that the canopy imposes a confinement of the flow with a threshold effect in λ_p , below which the flow structures are not constrained by the canopy geometry. In order to investigate the characteristics of coherent

motions driving the wall-normal exchanges, namely sweeps and ejections, co-spectra $-k_x k_y S(u, w)$ in plane z_1 are investigated (figures 6, top row). The ridge corresponding to the most energetic scales follows the same law $\lambda_x \propto \lambda_y^2$, confirming their large-scale interactions with LSMs. In the case of $\lambda_p = 25\%$ and 44.4% , the co-spectra $S(u, w)$ show a large energy maximum resulting in a flatter or even a double-peaked (when $\lambda_p = 25\%$) one-dimensional co-spectra, a feature also noticed for $S(u, u)$. This confirms the organization of ejections and sweeps within streaky LSMs. Overall, the energy spike associated with interactions between u and w velocity components occurs at decreasing scales when the canopy becomes denser. Since the spectra associated with u were essentially identical for the three canopy densities, such a trend points to smaller and narrower wall-normal motions (w component) interacting with the LSMs when inside the roughness sublayer.

CONCLUSIONS

The influence of the canopy geometry on the spatial organisation of the flow is investigated by addressing the presence of the typical types of coherent structures known to exist in turbulent boundary layers, such as VLSMs and LSMs, but also smaller scale structures related to the presence of sweeps and ejections. The present study shows that, overall, the characteristics of the large-scales whose footprints appear in the velocity components u and v , are not affected by the change of canopy configuration. In particular, the coexistence of VLSMs, LSMs, the later being characterized by their self-similar behaviour, has been demonstrated. In the logarithmic layer, this population of coherent structures is in agreement with that of smooth-wall boundary layers. Investigation of the two-dimensional spectra obtained in the RSL clearly shows the superimposition of two types of energetic structures, one related to the VLSMs identified in the logarithmic region and above and another one corresponding to LSMs with self-similar features. The main charac-

teristics of these structures who leave their imprint in the streamwise and spanwise velocity components were found to be independent of the roughness packing density. However, through the investigation of the spectra of w and the co-spectra between u and w , which relates to the sweep and ejection coherent structures, dynamics of wall-normal motions was found to depend on the roughness spatial arrangement. Their most energetic scales appear to be of the order of the canopy height and to decrease with increasing packing density. No controlling parameter linking the canopy morphology and the relevant scales in the wall-normal dynamics has been yet identified. Instead, a confinement effect of the flow was observed for the densest configuration, suggesting a threshold in terms of canopy density: a more or less sparse canopy arrangement enables or constrains the development of the shear layers emanating from the roughness obstacles and the penetration of the boundary layer LSMs closer to the wall.

REFERENCES

- Baars, W. J., Hutchins, N. & Marusic, I. 2017 Reynolds number trend of hierarchies and scale interactions in turbulent boundary layers. *Phil. Trans. R. Soc. A* **375**, 20160077.
- Basley, J., Perret, L. & Mathis, R. 2018 Spatial modulations of kinetic energy in the roughness sublayer. *J. Fluid Mech.* **850**, 584–610.
- Grimmond, C. S. B. & Oke, T. R. 1999 Aerodynamic properties of urban areas derived from analysis of surface form. *Journal of Applied Meteorology* **38**, 1262–1292.
- Jiménez, J. 2004 Turbulent flows over rough walls. *Ann Rev Fluid Mech.* **36**, 173–196.
- Perret, L., Basley, J., Mathis, R. & Piquet, T. 2019 Atmospheric boundary layers over urban-like terrains: influence of the plan density on the roughness sublayer dynamics. *Boundary-Layer Meteorol.* **170** (2), 205–234.